NASA TECHNICAL NOTE

NASA TN D-7759

NASA TN D-7759

WIND-TUNNEL TESTS OF MODIFIED CROSS, HEMISFLO, AND DISK-GAP-BAND PARACHUTES WITH EMPHASIS IN THE TRANSONIC RANGE

by Jerome T. Foughner, Jr., and William C. Alexander

Langley Research Center
Hampton, Va. 23665

NATIONAL AERONAUTICS AND SPACE ADMINISTRATION • WASHINGTON, D. C. • NOVEMBER 1974

1. Report No.	2. Government Accession No.	3. Recipient's Catalog No.
NASA TN D-7759		

4. Title and Subtitle	5. Report Date
WIND-TUNNEL TESTS OF MODIFIED CROSS, HEMISFLO, AND DISK-GAP-BAND PARACHUTES WITH EMPHASIS IN THE TRANSONIC RANGE	November 1974
	6. Performing Organization Code

7. Author(s)	8. Performing Organization Report No.
Jerome T. Foughner, Jr., and William C. Alexander	L-9421
	10. Work Unit No. 501-22-04-01
9. Performing Organization Name and Address	11. Contract or Grant No.
NASA Langley Research Center Hampton, Va. 23665	
	13. Type of Report and Period Covered
12. Sponsoring Agency Name and Address	Technical Note
National Aeronautics and Space Administration Washington, D.C. 20546	14. Sponsoring Agency Code

15. Supplementary Notes

William C. Alexander is associated with Goodyear Aerospace Corporation.

16. Abstract

Transonic wind-tunnel studies were conducted with modified cross, hemisflo, and disk-gap-band parachute models in the wake of a cone-cylinder shape forebody. The basic cross design was modified with the addition of a circumferential constraining band at the lower edge of the canopy panels. The tests covered a Mach number range of 0.3 to 1.2 and a dynamic pressure range from 479 N/m^2 (10 lbf/ft^2) to 5746 N/m^2 (120 lbf/ft^2). The parachute models were flexible textile-type structures and were tethered to a rigid forebody with a single flexible riser. Different size models of the modified cross and disk-gap-band canopies were tested to evaluate scale effects. Model reference diameters were 0.30, 0.61, and 1.07 meters (1.0, 2.0, and 3.5 ft) for the modified cross; and nominal diameters of 0.25 and 0.52 meter (0.83 and 1.7 ft) for the disk-gap-band; and 0.55 meter (1.8 ft) for the hemisflo. Reefing information is presented for the 0.61-meter-diameter cross and the 0.52-meter-diameter disk-gap-band. Results are presented in the form of the variation of steady-state average drag coefficient with Mach number. General stability characteristics of each parachute are discussed. Included are comments on canopy coning, spinning, and fluttering motions.

17. Key Words (Suggested by Author(s))	18. Distribution Statement
Parachutes Transonic data Wind-tunnel tests	Unclassified – Unlimited STAR Category 02

19. Security Classif. (of this report)	20. Security Classif. (of this page)	21. No. of Pages	22. Price*
Unclassified	Unclassified	36	$3.25

*For sale by the National Technical Information Service, Springfield, Virginia 22151

WIND-TUNNEL TEST OF MODIFIED CROSS, HEMISFLO, AND DISK-GAP-BAND PARACHUTES WITH EMPHASIS IN THE TRANSONIC RANGE

By Jerome T. Foughner, Jr., and William C. Alexander*
Langley Research Center

SUMMARY

A wind-tunnel investigation was conducted to determine the drag and stability characteristics through the transonic speed range of modified cross, hemisflo, and disk-gap-band parachutes in the wake of a cone cylinder. The tests covered a Mach number range of 0.3 to 1.2 and a dynamic pressure range from 479 N/m^2 (10 lbf/ft^2) to 5746 N/m^2 (120 lbf/ft^2). The basic cross design was modified with the addition of a circumferential constraining band at the lower edge of the canopy panels. Different size models of the modified cross and disk-gap-band parachutes were tested to evaluate scale effects. The modified cross parachute models had reference diameters of 0.30, 0.61, and 1.07 meters (1.0, 2.0, and 3.5 ft). Nominal diameters of the disk-gap-band models were 0.25 and 0.52 meter (0.83 and 1.7 ft). The hemisflo parachute nominal diameter was 0.55 meter (1.8 ft). In addition, one model each of the cross and the disk-gap-band parachutes was tested in a reefed condition.

In the compressible speed range (above Mach 0.6) all parachutes experienced canopy cyclic breathing and suspension line flutter. The modified cross and the disk-gap-band parachutes experienced significant changes in inflated canopy size and shape; these changes resulted in a gradual reduction in drag coefficient as the Mach number increased. The hemisflo canopy parachute did not experience noticeable changes in size and shape when operating above Mach 0.6. The drag performances of the modified cross and disk-gap-band parachutes of different sizes were essentially equal and indicated that there were no significant scale effects within the size ranges of the test. In general, for tests in the incompressible speed range, Mach 0.3 to 0.6, the parachutes appeared to be fully inflated, were free of canopy breathing and flutter, and exhibited good angular stability characteristics. A drag performance variation observed in this speed range was attributed to initial elongation of tension members (and a resulting canopy size increase) as the test dynamic pressure was increased.

---

*William C. Alexander is associated with Goodyear Aerospace Corporation.

INTRODUCTION

There is considerable continued interest in the use of parachutes as decelerators for a variety of aerospace applications, such as the landing of the Viking spacecraft on Mars, the returning of the space shuttle solid rocket boosters for later reuse, and the delivery of military payloads. Many of these applications require that the parachutes be deployed at high speeds and at various dynamic pressure levels. A literature survey of available documented data concerning parachute performance revealed a lack of drag and stability data in the transonic speed range for current system configurations. The primary purpose of this investigation was to obtain parachute drag and stability data in the high subsonic and transonic Mach number range for three parachute configurations: the modified cross, hemisflo, and disk-gap-band types. (See fig. 1.) A second purpose was to evaluate scale effects by testing different size models of the modified cross and disk-gap-band parachutes.

Wind-tunnel data that are applicable to this investigation include references 1 and 2 for the basic cross parachute design, reference 3 for the hemisflo, and reference 4 for the disk-gap-band. No documented data were found for the modified cross parachute as tested herein. The variation in the effects of the cone-cylinder forebody on test results was minimized by changing the forebody scale to maintain a constant ratio between forebody diameter and parachute diameter for all tests. Reefing data were also obtained on specific cross and disk-gap-band models. Some of the results of this investigation have been presented and correlated with previously published subsonic and supersonic model wind-tunnel data of reference 5.

The tests were conducted in the Langley transonic dynamics tunnel over a Mach number range of 0.3 to 1.2 and a dynamic pressure range from 479 N/m^2 (10 lbf/ft^2) to 5746 N/m^2 (120 lbf/ft^2). The parachute models were textile-type structures and were tethered to the rigid forebody with a single textile riser.

SYMBOLS

The principal measurements and calculations presented in this paper were made in U.S. Customary Units and were converted to the International System of Units (SI) for presentation. In some cases both SI and Customary Units are used. When this is done, the SI units are stated first and Customary Units afterwards in parentheses. When no units are stated, the ones used are those given in the symbol list.

$C_{D,o}$ drag coefficient based on nominal canopy surface area, F/qS_o

D_N reference diameter for cross parachute defined as panel length, m

D_o nominal diameter, $\left(\frac{4S_o}{\pi}\right)^{1/2}$, m

D_p projected diameter (measured from film), m

d maximum diameter of forebody, m

F drag force, N

ℓ_s length of suspension line, in model diameters

M free-stream Mach number

q free-stream dynamic pressure, N/m^2

S_o nominal surface area of parachute canopy including geometric open areas within borders of cloth material (for the cross parachute, $S_o = 2D_N W - W^2$), m^2

W panel width of cross parachute, m

x trailing distance of skirt edge of parachute canopy behind the forebody base, m

z number of suspension lines

λ_g geometric canopy porosity, percent

λ_m mechanical porosity (permeability of fabric), $(m^3/min)/m^2$, at 1.27 cm H_2O differential pressure

Model code:

For clarity and brevity each parachute model is designated by an alphanumeric code. The first letter of the code refers to the type of parachute, C for cross, D for disk-gap-band, and H for hemisflo. A digit is used to differentiate between models of the same type, for example, C1 and C2. In some instances a third character is used

to indicate special features of the model; R indicates reefed, and M indicates an increased ratio of parachute nominal diameter to forebody base diameter.

APPARATUS AND TESTS

Unreefed and reefed parachute models were tested behind a basic cone-cylinder forebody in order to keep the results general, yet realistic in nature. A schematic drawing of the forebody and the forebody-parachute configuration is presented in figure 2. The cone-cylinder was supported in the wind tunnel by the cable mount system as illustrated in figure 3. The mount system was effective in holding the forebody rigid throughout the Mach number and dynamic pressure range of the studies.

Geometric properties of the parachute models are summarized in table I. The parachutes were placed 9.0 to 11.0 forebody diameters downstream for the purpose of minimizing forebody wake effects. Different model sizes were tested to obtain an indication of scale effects. To preserve the parachute to forebody diameter ratio, the forebody diameter was increased proportionally to the parachute diameter increase. This ratio was kept in the range of 4.2 to 5.1, except for one disk-gap-band configuration where the ratio was 8.3. In the design and construction of the modified cross and disk-gap-band parachute models, suspension line lengths, fabric permeability, and geometric porosity were kept the same. In addition, for the disk-gap-band models, the number of suspension lines was kept the same.

The purpose for selecting a flexible parachute structure was to simulate the inflated size and shape changes that occur over a given range of flight conditions. It is noted that these two-body tests are considered to be infinite mass-type tests since the payload was held in a fixed position and the flow velocity was constant.

Test Parachutes

Modified cross parachute.- Specifications of each cross parachute are presented in table II. The basic cross canopy has two panels that are placed at right angles to each other; these panels overlap and form the cross. By definition the reference diameter is equal to the panel length, and panel width for these models was 0.26 times the panel length. The basic cross was modified for this investigation with the addition of a constraining band. The constraining band was sewn across the panel hems; thus, the two rectangular panels were connected in a manner similar to that of a skirt band. (See fig. 1.) Constraining band lengths are given in table II. As mentioned previously, different sizes of the modified cross parachutes were tested (table I, code C1, C2, and C3, see symbol list for discussion of code). The reference diameters were 0.30, 0.61, and 1.07 meters (1.0, 2.0, and 3.5 ft). In addition the 0.61-meter-diameter model was

tested in a reefed condition (code C2R) with a reefing line length of 0.52 meter. This reefing line was installed inside the panel hem by means of 12 reefing rings. The 0.30-meter model and the 0.61-meter model had 12 suspension lines. The 1.07-meter model had 16 suspension lines. The suspension line length for all models was 1.4 times the reference canopy diameter $(1.4D_N)$. The structural strength of textile components was scaled (by approximately the square of the model diameter ratio) as the model size increased. (See table II.)

Hemisflo parachute.- Specifications of the hemisflo parachute are presented in table III. This canopy is hemispherical in shape and may be described as an extended skirt-ribbon canopy. The reference diameter was 0.55 meter (1.8 ft). The model had 16 suspension lines and a suspension line length of $1.74D_O$. Geometric canopy porosity was 9.4 percent.

Disk-gap-band parachute.- Specifications of the disk-gap-band parachutes are presented in table IV. This canopy consists of a disk, an annular opening, the "gap," and an annular band. Two disk-gap-band parachute sizes were tested (code D1 and D2). Their diameters were 0.25 and 0.52 meter (0.83 and 1.7 ft). The 0.52-meter-diameter model was also tested in a reefed condition (code D2R). The reefing line length was 0.46 meter. The reefing line was installed inside the band leading edge by means of 18 reefing rings. Each parachute had a design geometric porosity of 12.5 percent and had 18 suspension lines. The length of each line was equal to the nominal diameter D_O. The ratio of parachute nominal diameter to forebody base diameter was increased to 8.3 for one configuration by decreasing the forebody diameter (code D2M). This configuration was included to provide information applicable to the Viking Mars Lander Project.

Wind Tunnel

The tests were conducted in the Langley transonic dynamics tunnel which has a 4.9-meter square (16-foot) test section with cropped corners and is a return-flow, variable-pressure, slotted-throat wind tunnel. The cross-sectional area of the test section is 23 meters^2 (248 ft^2). The tunnel is capable of operation at stagnation pressures from 0.1 atmosphere to slightly above atmospheric pressure and at Mach numbers from 0 to 1.2. Mach number and dynamic pressure can be varied independently with either air or Freon used as a test medium; however, the tests were conducted using air as the test medium. A more complete description of the wind tunnel is given in reference 6.

Instrumentation

Parachute axial-force measurements were obtained with a small tensiometer located in the riser line. A 3-kHz amplitude-modulated carrier amplifier was used to

provide the excitation voltage for the tensiometer. An indicating millivolt servo potentiometer was used to monitor the tensiometer output signal. An analog-to-digital converter was used to obtain this output signal on a tabulator and a card punch. This output was proportional to the average static drag. The output signal of the carrier amplifier was also passed directly to a frequency-modulated tape recorder.

Three motion-picture cameras (400 frames per second) were used to provide a visual record of canopy motions. A television tape of each test was also made. In addition, the test parachute was photographed during each data run with a single-frame sequence-type camera.

Tests

Procedure.- The parachute model to be tested was attached to the cone-cylinder forebody (fig. 3) before initiation of wind-tunnel operations. When the model was in place and all instrumentation was set for the tests, a static calibration was made of the output of the tensiometer. For this calibration, known static loads were applied and the corresponding output of the strain-gage bridge was measured. Pretest and posttest calibrations were taken for each parachute model. The tunnel was started, and the stagnation pressure and speed were set to give a desired Mach number and dynamic pressure. For each data run the tensiometer output was tabulated and a 1-minute time history recorded on the analog tape recorder. Tunnel stagnation temperature and pressure and static pressure were tabulated for each data run.

Test conditions.- The tests covered a Mach number range from 0.3 to 1.2 and dynamic pressures ranged from 479 N/m^2 (10.0 lbf/ft^2) to 5746 N/m^2 (120 lbf/ft^2). Runs were made over a dynamic pressure range for the code D2M model at a constant Mach number of 0.6 in order to check the effect of Reynolds number on canopy performance data.

Accuracy.- The drag coefficient $C_{D,o}$ was defined as the force measured divided by the product of free-stream dynamic pressure and the nominal surface area of the parachute canopy. The nominal surface areas of all test parachutes are presented in table I. Based on the accuracy of the tensiometer and the tunnel flow property measurements, the drag coefficients are estimated to have a maximum uncertainty of ±0.011. Blockage ratio values, defined as the inflated parachute canopy cross-sectional area divided by the tunnel test-section cross-sectional area, range from 0.05 percent to 0.68 percent for the various size test parachutes. No corrections for blockage effects or for wind-tunnel-wall interference were applied to the data. It is estimated that measurements of the maximum canopy projected diameter (obtained from the photographic film) have a 1-percent accuracy.

RESULTS AND DISCUSSION

The basic parachute performance data are presented in the form of the variation of steady-state average drag coefficient with Mach number. General stability characteristics of each parachute are discussed. These discussions include comments (based on viewing the high-speed motion pictures) on canopy coning, spinning, and fluttering motions.

Modified Cross Parachute

The drag-coefficient results for the three sizes of modified cross parachute models as a function of Mach number are given in figure 4. Representative canopy photographs are shown in figure 5. Note that a constraining band was used with each model. From figure 4 it may be seen that the drag coefficient for the three parachutes decreased about 20 percent when the Mach number increased from 0.6 to 1.1. In this Mach number range there appears to be no significant difference in drag performance for the three different size models. At low speeds (Mach 0.3 to 0.6) the values shown in figure 4 range from 0.50 to 0.65. A reason for this variation in drag coefficient is discussed in the section "Observations Concerning Model Textile Properties at Low Dynamic Pressures."

The low-speed ($M < 0.3$) drag coefficient values for a 1.07-meter model of reference 1 range from 0.65 to 0.70. The reference 1 model was a basic cross parachute (no constraining band) with the same geometric properties of the code C3 model except for a smaller forebody diameter $\left(D_N/d = 11.4,\ x/d = 16\right)$. The lower drag coefficient values obtained in this investigation (0.5 to 0.65) are attributed primarily to the presence of the constraining band.

The models were very stable in terms of coning stability (less than 3^o amplitude) throughout the Mach number range of the tests. The 0.30-meter- and 0.61-meter-diameter models spun throughout the tests. The spin rate was between 50 and 100 revolutions per second for the 0.30-meter model and between 25 and 55 revolutions per second for the 0.61-meter model. The 1.07-meter-diameter model did not spin.

As the Mach number was increased to approximately Mach 0.6, the three model canopies were free of flutter and breathing. As the Mach number was increased above 0.6, all models began to flutter and breathe, and canopy inflated shape and size changes were observed. Figure 6 shows the 1.07-meter model at both Mach 0.34 and 0.77. In figure 6(a) the constraining band is in tension and in figure 6(b) the band is slack. This condition indicates the skirt leading-edge diameter is smaller in figure 6(b). The lack of tension in the constraining band at Mach 0.77 allowed the ends of the panels to perform an oscillatory scissoring motion. This motion was superimposed on the basic radial

oscillatory breathing motion of the canopy panels. During tests of the 0.30-meter and 0.61-meter models above Mach 0.6, the observed canopy motions were the combined effect of radial breathing and spinning. A review of the motion pictures revealed that even though these models were spinning, canopy shape changes did occur similar to those of the 1.07-meter model.

A cross parachute model 0.61 meter in diameter was tested with a reefing line length of 0.52 meter. This length results in a ratio of reefed diameter to referenced diameter of 0.27. The drag coefficient as a function of Mach number is shown in figure 7. A representative canopy photograph is shown in figure 8. Comparative results of the drag-coefficient values between the reefed model (fig. 7) and the unreefed modified model (fig. 4) at a Mach number of approximately 0.5 show the ratio of respective drag coefficients to be 0.52. The ratio of the frontal areas of the measured inflated model was 0.59. The model did spin (at 6 to 13 revolutions per second) throughout the test. The inflated shape and the drag coefficient both remained relatively constant over the Mach number range of the tests. Slight canopy breathing and flutter were observed at operating speeds above Mach 0.7.

Hemisflo Parachute

In figure 9, the drag coefficient variation for the hemisflo model is presented as a function of Mach number. A representative canopy photograph of the hemisflo model is shown in figure 10. The model did not spin and exhibited very little coning motion throughout the Mach number range. Below Mach 0.6, the model remained relatively motionless and constant in terms of fully inflated shape. Above Mach 0.6, slight canopy breathing and flutter were observed. The 0.55-meter-diameter model (code H1) did not change shape and size as the Mach number was increased above Mach 0.6. The resulting drag coefficients, as indicated in figure 9, were relatively constant.

Disk-Gap-Band Parachute

The drag coefficient for the disk-gap-band models is presented in figure 11 as a function of Mach number. Representative photographs are shown in figure 12. Three tests were conducted on two model sizes. The two models were 0.25 meter and 0.52 meter in diameter. Throughout the Mach number range, the 0.25-meter-diameter model (code D1) was very stable in terms of coning stability. As the Mach number was increased above Mach 0.6, there was a significant change in inflated shape (became less blunt) and the model began to flutter and breathe. This shape change became more prominent as the Mach number was increased, and a reduction in drag was observed.

For one test the 0.51-meter-diameter model (code D2) was exposed to conditions similar to those experienced by the 0.25-meter-diameter model. The ratio of trailing

distance to forebody diameter (x/d) and the ratio of parachute nominal diameter to forebody diameter (D_o/d) were kept the same. To satisfy the requirement of the same ratio of trailing distance to forebody diameter, the riser line length was doubled for the 0.52-meter-diameter model (code D2). As the Mach number was increased to Mach 0.6, the code D2 was very stable (in terms of coning). It did not spin, and no significant shape change occurred. Above Mach 0.6 the shape changed and canopy flutter and breathing occurred. With additional increase in Mach number, the model experienced large-amplitude coning excursions. These excursions resulted in the 0.52-meter-diameter model (code D2) having a high average angle of attack. As a consequence, higher and relatively constant drag values were obtained between Mach 0.6 and 1.1. (See fig. 11.) It is not known what caused the large-amplitude coning excursions of the code D2 model; however, the increased riser line length may have been a contributing factor. Tests of this configuration were not repeated. However, a second test was conducted with the 0.52-meter-diameter model to provide information for Viking Mars Lander application. The development of the Viking parachute configuration (disk-gap-band) is summarized in reference 7. The 0.52-meter configuration (code D2M) had a shorter riser length and a smaller forebody. This model configuration was stable and performed in a manner similar to the 0.25-meter configuration (code D1) throughout the Mach number range. (See fig. 11.)

The average subsonic drag-coefficient value for the disk-gap-band canopy as seen from figure 11 is 0.37. This value is less than a subsonic value of 0.52 for disk-gap-band canopies as given in reference 4. The subsonic drag-coefficient value of reference 4 was obtained on a 1.67-meter-diameter model. This model had 32 suspension lines, and a geometric porosity of 12.5 percent. The present models have 18 suspension lines, and a geometric porosity of 12.5 percent. The lower drag coefficients in the present tests are believed to be due primarily to the fact that the present models had fewer suspension lines than the model of reference 4.

Reefed disk-gap-band.- A 0.52-meter-diameter (code D2R) disk-gap-band parachute was tested with a reefing line length of 0.41 meter, giving a ratio of reefed diameter to nominal diameter ratio of 0.25. The drag coefficient variation with Mach number is shown in figure 13, and a representative canopy photograph is shown in figure 14. Considerable coning motion, up to 10°, was observed throughout the Mach number range. Canopy breathing and flutter was observed above Mach 0.6. At a Mach number of 0.6 the drag coefficient of the reefed configuration (fig. 13) was 70 percent of the unreefed configuration (fig. 11). The ratio of the measured frontal areas of the inflated model was 0.77.

Reynolds number effect.- The effect of Reynolds number and of dynamic pressure on the drag coefficient at a constant Mach number of 0.6 is presented in figure 15. The

configuration is a 0.52-meter (code D2M) disk-gap-band parachute (x/d = 10.8 and D_o/d = 8.3). The drag coefficient is seen to be independent of Reynolds number and dynamic pressure over the range of the tests.

Parachute Flexibility Effects On Drag

Typical wind-tunnel results show that the drag coefficients of rigid blunt-body models (such as a sphere or a flat plate) increase by a factor of about 1.5 to 2.0 when the Mach number increases from 0.6 to 1.0. (See ref. 8.) Since the models of reference 8 were metal models, the frontal area presented to the flow was constant. Because of their basic shapes, the boundary-layer flow separation occurred at nearly the same location on the model independent of Mach number, namely, near the maximum diameter. With a constant flow separation point, the variations in force coefficients are attributed directly to changes in pressures with Mach number. These physical changes in pressures above Mach 0.6 are attributed to compressibility effects.

The test results presented in figures 4, 9, and 11 reveal no trend of increasing drag coefficients with increasing Mach number above a Mach number of 0.6. Actually, the drag coefficients of the modified cross and the disk-gap-band models are seen to decrease with increasing Mach number above 0.6. This difference in performance of rigid and flexible parachute models can be attributed to the difference in the structure. A parachute is made of flexible textile tension members. The canopy is porous, and the total structure (canopy and suspension lines) is free to elongate and change size and shape.

Canopy Size and Shape Changes

Results from the tests of the modified cross and the disk-gap-band models (figs. 4 and 11) indicate a downward trend in drag coefficient with increasing Mach number above Mach 0.6. As previously stated, a size and shape change was observed when operating above Mach 0.6. To indicate the magnitude of model geometry change relative to the change in drag-coefficient values, estimates of the canopy projected diameter were made from the film. The ratio of measured inflated diameter to reference or nominal diameter squared, $(D_p/D_o)^2$ or $(D_p/D_N)^2$, as a function of Mach number is given in figure 16 for the code C2, H1, and D1 models. The results indicate that the reduction in drag coefficient is correlated to the reduction in parachute inflated diameter for the modified cross (C2) and the disk-gap-band (D1). The hemisflo model inflated diameter (dashed lines in fig. 16) remains relatively constant. This result is in agreement with the drag coefficients observed for the hemisflo model in figure 9.

Canopy Configuration Effects on Size and Shape Changes

The conclusion that little change occurs in the size and shape of ribbon canopies (hemisflo) with increasing Mach number above 0.6 and that significant change occurs in the size and shape of cloth canopies (modified cross and disk-gap-band) with increasing Mach number above 0.6 is supported by the wind-tunnel results of rigid parachute models of reference 9. Average external and internal pressure coefficient data from reference 9 for a cloth canopy with zero porosity and for a ribbon canopy with geometric porosity (openness) is presented in table V. No significant pressure coefficient difference occurs on the rigid ribbon parachute between Mach 0.61 and Mach 1.19. Since there is no pressure difference for this configuration, it follows that for the flexible hemisflo ribbon model, the size and shape change would not occur over the indicated Mach number range. In contrast, table V data show a significant pressure difference for a rigid guide-surface (cloth-canopy type) model between Mach number 0.61 and 1.23. Thus, for the flexible modified cross and disk-gap-band type canopies, a size and shape change could occur over the indicated Mach number range. In summary, the significant size and shape change that occurred for the flexible cloth canopies with increasing Mach number above a Mach number of 0.6 is consistent with what might be expected from pressure distribution measurements made on rigid model canopies.

Observations Concerning Model Textile Properties at Low Dynamic Pressures

The wind-tunnel test procedure was such that as the Mach number increased, the dynamic pressure increased. Thus, initial canopy loading occurred at low Mach numbers and low dynamic pressures. At low speeds (Mach 0.3 to 0.6), the drag coefficient values of the modified cross parachutes presented in figure 4 varied from 0.50 to 0.65. In figure 17 the drag coefficients of the 0.30-meter-diameter (C1) and the 0.60-meter-diameter (C2) modified cross parachute models are presented as a function of dynamic pressure. As seen, low drag coefficient values occur at low dynamic pressures. A trend of increasing drag with dynamic pressure is noted, and then a leveling off of this trend is seen. At the low canopy loads it is believed that drag values are affected by the inherent structural properties of the textile fabric models. This result is supported by the results presented in figure 18 which show the drag coefficient as a function of drag load in normalized form for the C1 and C2 modified cross models. The normalized drag load is defined as the ratio of the measured drag load to the number of suspension lines z times suspension line strength. The initial increase in drag coefficient (fig. 18) is a result of the elongation of the tension members (such as braided suspension lines and constraining bands); this elongation results in an increase of canopy area. The slackness of the twist (of each individual cord) is removed with increase in load. Once

the initial slack is gone, further increase in load requires an elongation of the basic yarn, and this growth occurs at a smaller rate. As indicated in figure 18, the drag coefficients reach a constant level when the normalized drag load ratio is greater than 1.5 to 2.0 percent.

In summary, evidence is presented which shows that in the low-speed range (Mach 0.3 to 0.6) of this study the variation in drag coefficient is associated with dynamic pressure and the model textile properties. This condition occurs until a normalized drag load ratio of 1.5 to 2.0 percent is achieved.

SUMMARY OF RESULTS

Transonic wind-tunnel studies of modified cross, hemisflo, and disk-gap-band different size parachute models have been conducted in the wake of a cone-cylinder shaped forebody. The tests covered a Mach number range of 0.3 to 1.2 and a dynamic pressure range from 479 N/m^2 (10 lbf/ft^2) to 5746 N/m^2 (120 lbf/ft^2). Analyses of drag-force measurements and motion-picture data have indicated the following results:

1. In the transonic range above a Mach number of 0.6, the modified cross and the disk-gap-band models decreased in inflated size and shape with increasing Mach number; this decrease resulted in a corresponding drag loss. In addition, because the parachute was not fully inflated or continually under tension loads in this speed range, canopy breathing and line flutter occurred.

2. In the transonic range above a Mach number of 0.6, the hemisflo model did not change inflated size and shape. Therefore, the resulting drag coefficient values are relatively constant in this speed range.

3. In the transonic range above a Mach number of 0.6, the drag performance for both modified cross and disk-gap-band parachute models of different sizes indicates that the drag coefficients are independent of model diameter over the size range of the tests.

4. In the incompressible subsonic speed range, Mach 0.3 to 0.6, all parachutes appeared to be fully inflated, were free of canopy breathing and flutter, and exhibited good angular stability characteristics. An observed drag coefficient variation in this speed range is associated with initial elongation of tension members. Drag coefficients reach a constant level when the normalized drag load ratio is greater than 1.5 to 2.0 percent.

5. The drag coefficient for a disk-gap-band parachute model at a constant Mach number of 0.6 was independent of Reynolds number and dynamic pressure throughout the range of the tests.

6. For the reefed cross and disk-gap-band models, the drag values were related directly to the reduction in the reefed inflated projected area relative to unreefed model drag values and their corresponding projected areas.

Langley Research Center,
National Aeronautics and Space Administration,
Hampton, Va., September 3, 1974.

REFERENCES

1. Ludtke, W. P.: Effects of Canopy Geometry on the Drag Coefficient of a Cross Parachute in the Fully Open and Reefed Conditions for a W/L Ratio of 0.264. NOLTR 71-111, U.S. Navy, Aug. 20, 1971. (Available form DDC as AD 731 023.)

2. Niccum, R. J.; Haak, E. L.; and Gutenkauf, Robert: Drag and Stability of Cross Type Parachutes. FDL-TDR-64-155, U.S. Air Force, Feb. 1965. (Available from DDC as AD 460 890.)

3. Amer. Power Jet Co.: Performance of and Design Criteria for Deployable Aerodynamic Decelerators. ASD-TR-61-579, U.S. Air Force, Dec. 1963. (Available from DDC as AD 429 921.)

4. Bobbitt, P. J.; Mayhue, R. J.; Faurote, G. L.; and Galigher, L. L.: Supersonic and Subsonic Wind-Tunnel Tests of Reefed and Unreefed Disk-Gap-Band Parachutes. AIAA Paper No. 70-1172, Sept. 1970.

5. Alexander, William C.; and Foughner, Jerome T., Jr.: Drag and Stability Characteristics of High-Speed Parachutes in the Transonic Range. AIAA Paper No. 73-473, May 1973.

6. Yates, E. Carson, Jr.; Land, Norman S.; and Foughner, Jerome T., Jr.: Measured and Calculated Subsonic and Transonic Flutter Characteristics of a 45° Sweptback Wing Planform in Air and in Freon-12 in the Langley Transonic Dynamics Tunnel. NASA TN D-1616, 1963.

7. Steinberg, Sy; Siemers, Paul M., III; and Slayman Robert G.: Development of the Viking Parachute Configuration by Wind-Tunnel Investigation. J. Spacecraft, vol. 11, no. 2, Feb. 1974, pp. 101-107.

8. Hoerner, Sighard F.: Fluid-Dynamic Drag. Publ. by the author (148 Busteed Drive, Midland Park, New Jersey 07432), 1965.

9. Heinrich, H. G.; Ballinger, J. G.; and Ryan, P. E.: Pressure Distribution in Transonic Flow of Ribbon and Guide Surface Parachute Models. WADC Tech. Note 59-32, DDC Doc. No. AD 210 257, Feb. 1959.

TABLE I.- SUMMARY OF MODEL GEOMETRIC PROPERTIES

Configuration	Test code	D_N	S_o	d	D_N/d	x/d	ℓ_s	z	λ_m	λ_g
Cross[1]	C1	0.30	0.042	0.06	5.0	10.8	1.4	12	63.3	---
Cross[2]	C2	0.61	0.170	0.12	5.0	10.3	1.4	12	63.3	---
Cross	C3	1.07	0.520	0.21	5.1	8.7	1.4	16	63.3	---
Cross – reefed	C2R	0.61	0.170	0.12	5.0	10.9	1.4	12	63.3	---

Configuration	Test code	D_o	S_o	d	D_o/d	x/d	ℓ_s	z	λ_m	λ_g
Hemisflo	H1	0.55	0.230	0.12	4.5	9.7	1.7	16	---	9.4
Disk-gap-band	D1	0.25	0.051	0.06	4.2	10.4	1.0	18	34.7	12.5
Disk-gap-band[3]	D2	0.52	0.203	0.12	4.2	10.5	1.0	18	34.7	12.5
Disk-gap-band	D2M	0.52	0.203	0.06	8.3	10.8	1.0	18	34.7	12.5
Disk-gap-band – reefed	D2R	0.52	0.203	0.12	4.2	10.5	1.0	18	34.7	12.5

[1]All basic cross parachutes modified with constraining band.

[2]Swivel failed (M = 0.88, q = 2740 N/m^2).

[3]Swivel failed (M = 1.09, q = 5747 N/m^2).

TABLE II.- MODEL SPECIFICATIONS FOR CROSS PARACHUTES

Item	Model code		
	C1	C2 / C2R	C3
Panel:			
Length, m (By definition = D_N)	0.30	0.61	1.07
Width-to-length ratio	0.26	0.26	0.26
Panel tape:			
Width, cm	0.64	0.95	2.84
Strength, N	173	890	4 893
Cloth:			
Mass, g/m^2	129	129	129
Strength, N/m	3.32	3.32	3.32
Constraining band:			
Strength, N	1334	4 448	10 231
Length, m	0.58	1.17 / ---	2.05
Width, cm	------	1.27	1.91
Suspension line:			
Strength, N	222	890	2 446
Length, cm	43	85	149
Riser:			
Strength, N	1334	4 448	8 896
Length, m	0.24	0.39 / 0.47	0.33
Longitudinal reinforcements:			
Number	12	12	16
Strength, N	173	890	2 224
Width, cm	0.64	0.95	1.42
Reefing line:			
Strength, N	------	10 231	-------
Length, m	------	0.52	-------
Width, cm	------	1.91	-------

Materials	Model code		
	C1	C2 and C2R	C3
Canopy cloth	Dobby taffeta weave, nylon		
Suspension line	Cord, nylon MIL-C-17183, Revision B	Cord, nylon MIL-C-7515D, Type XV	Cord, nylon MIL-C-7515D, Type II
Longitudinal reinforcement	Tape, nylon MIL-T-5608C, Type I	Tape, nylon MIL-T-5038, Type III	Tape, nylon MIL-T-5038, Type V
Panel tape	Tape, nylon MIL-T-5608C, Type I	Tape, nylon MIL-T-5038, Type III	Tape, nylon MIL-T-5038, Type IV
Constraining band	Cord, nylon MIL-C-7515D, Type XI	Web, nylon MIL-W-5625	Web, nylon MIL-W-5625
Riser	Cord, nylon MIL-C-7515D, Type XI	Cord, nylon MIL-C-7515D, Type IV	Cord, nylon MIL-C-7515D, Type VI
Reefing line	----------	Web, nylon MIL-W-5625	----------

TABLE III.- MODEL SPECIFICATIONS FOR HEMISFLO PARACHUTE

Item	Model code – H1
Nominal diameter, m	0.55
Vent diameter, cm	7.26
Gore:	
Height, cm	31.9
Width at skirt, cm	6.25
Width at equator, cm	6.55
Width at vent, cm	1.73
Radial ribbons:	
Width, cm	0.64
Strength, N	173
Vertical ribbons:	
Number per gore	3
Width, cm	0.32
Strength, N	356
Horizontal ribbons:	
Number	42
Spacing, cm	0.04
Width, cm	0.64
Strength, N	173
Vertical band:	
Width, cm	0.64
Strength, N	222
Skirt band:	
Width, cm	0.64
Strength, N	222
Suspension lines:	
Length, cm	94
Strength, N	445
Riser line:	
Strength, N	4448
Length, cm	0.23

Materials	Model code – H1
Suspension line	Cord, nylon MIL-C-5040D, Type I
Radial ribbons	Tape, nylon MIL-T-5608C, Type I
Vent bands	Shroud, nylon MIL-C-5040D, Type II (cords removed)
Horizontal ribbons	Tape, nylon MIL-T-5608C, Type I
Vertical ribbons	Tape, Nomex
Model risers	Cord, nylon MIL-C-7515D, Type IV

TABLE IV.- MODEL SPECIFICATIONS DISK-GAP-BAND PARACHUTES

Item	Model code	
	D1	D2, D2M, and D2R
Canopy diameter D_N, m	0.25	0.52
Vent diameter, cm	2.1	4.2
Gap width, cm	25.4	50.8
Reinforcement strength, N:		
Vent and disk edge cord	445	445
Inner and outer band edge	445	445
Cloth mass, g/m^2	76.5	76.5
Cloth strength, N/m	1.40	1.40
Gore height, cm	13.3	26.7
Maximum gore width, cm	3.3	6.6
Suspension line:		
Length, cm	25.4	50.8
Strength, N	445	890
Riser line strength, N	2446	4448
Riser line strength, m	0.38	0.76, 0.15, 0.76
Reefing line strength, N	------	10231
Reefing line length, m	------	0.46

Materials	Model code	
	D1	D2, D2M, and D2R
Canopy cloth	Square weave, dacron (Stern and Stern no. 15004)	
Suspension line	Cord, nylon MIL-C-5040D, Type I	Cord, nylon MIL-C-7515D, Type XV
Riser	Cord, nylon MIL-C-5040D, Type III	Cord, nylon MIL-C-7515D, Type IV
Reefing line	----------	Cord, nylon MIL-C-7515D, Type XI
Canopy edge reinforcements	Shroud, nylon MIL-C-5040D, Type III	

TABLE V.- PRESSURE DISTRIBUTION OF RIGID MODEL CANOPIES IN TRANSONIC FLOW (DATA FROM REF. 9)

Mach number	Reference table no.	Average pressure coefficient		Pressure coefficient difference
		Internal	External	
Ribbon type canopy				
0.61	1	1.0632	-0.5397	1.6029
1.19	8	1.3586	-.2744	1.6330
Guide surface type canopy				
0.61	9	1.1323	-0.2500	1.3823
1.23	16	1.3970	-1.1000	2.5000

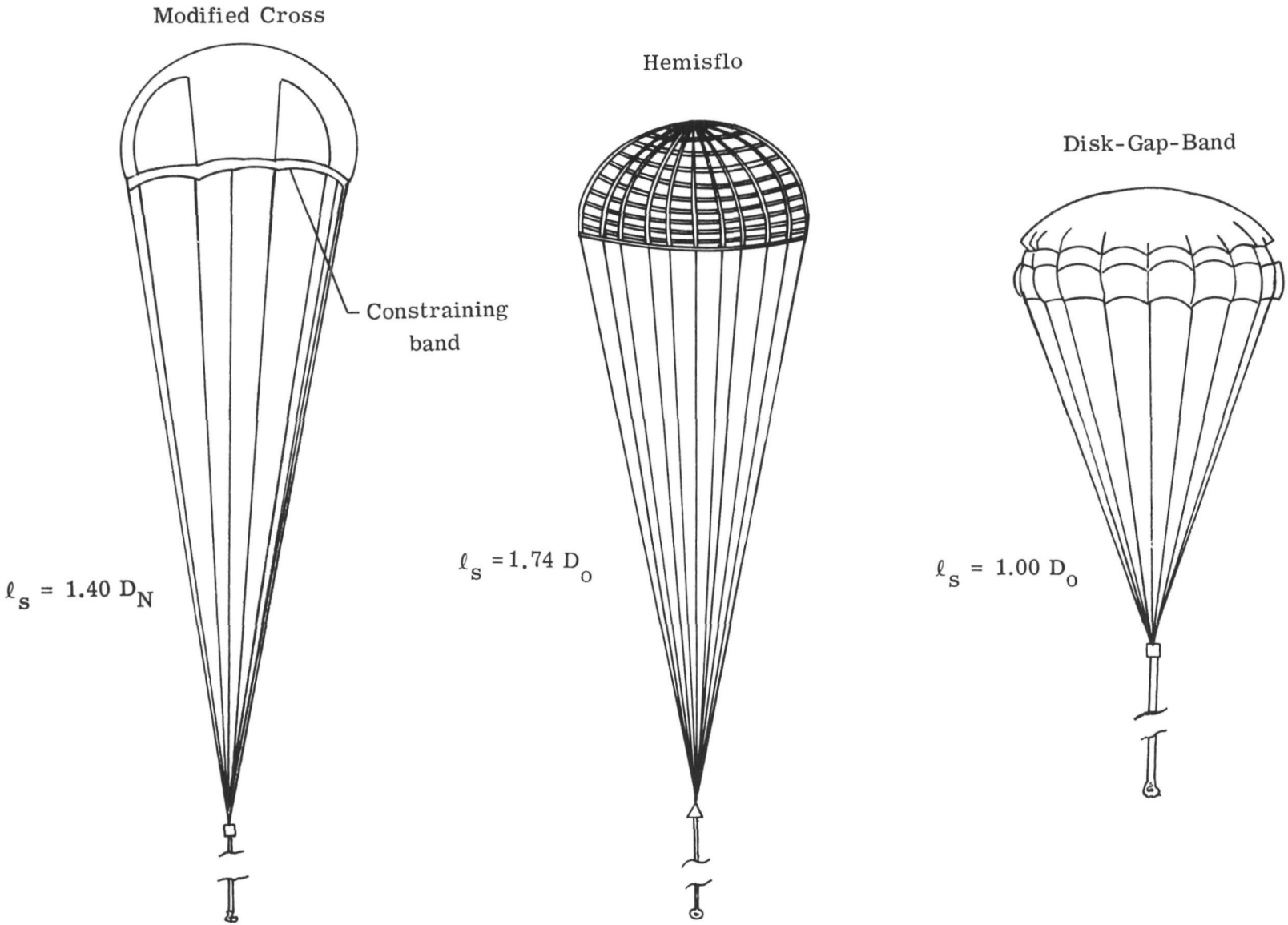

Figure 1.- Parachute configurations studied (not to scale).

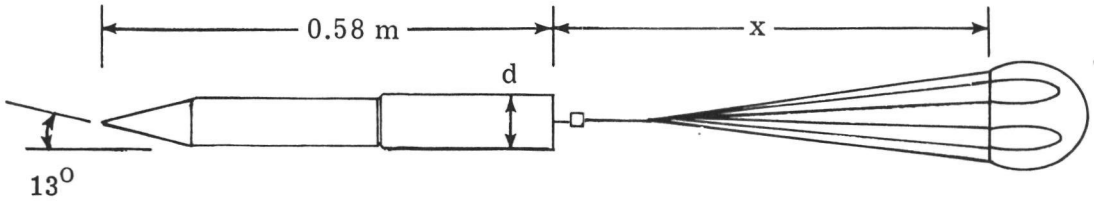

(a) Forebody "A" with typical parachute configuration.

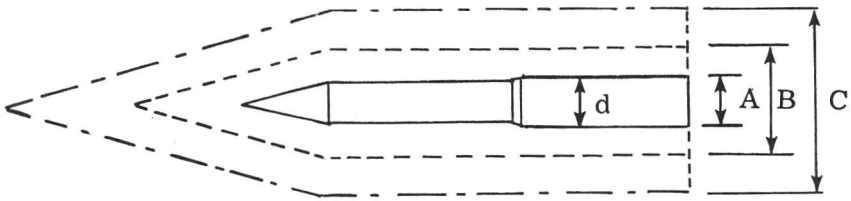

Forebody	Test code	d, m
A	C1, D1, D2M	0.06
B	C2, C2R, H1, D2, D2R	0.12
C	C3	0.21

(b) Forebody size variation.

Figure 2.- Schematic of model forebody configurations.

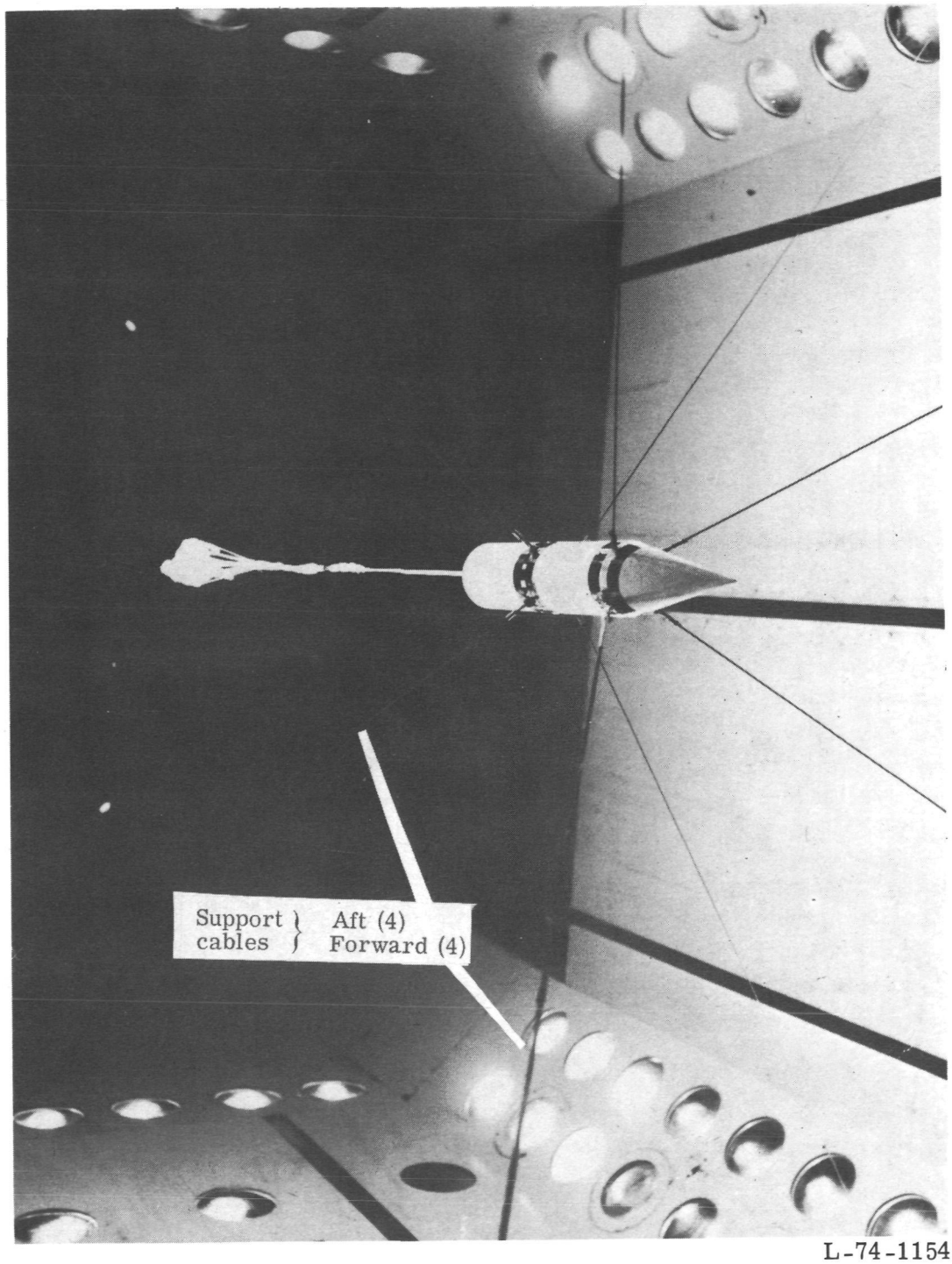

L-74-1154

Figure 3.- Cable mount system with configuration C3 prior to test.

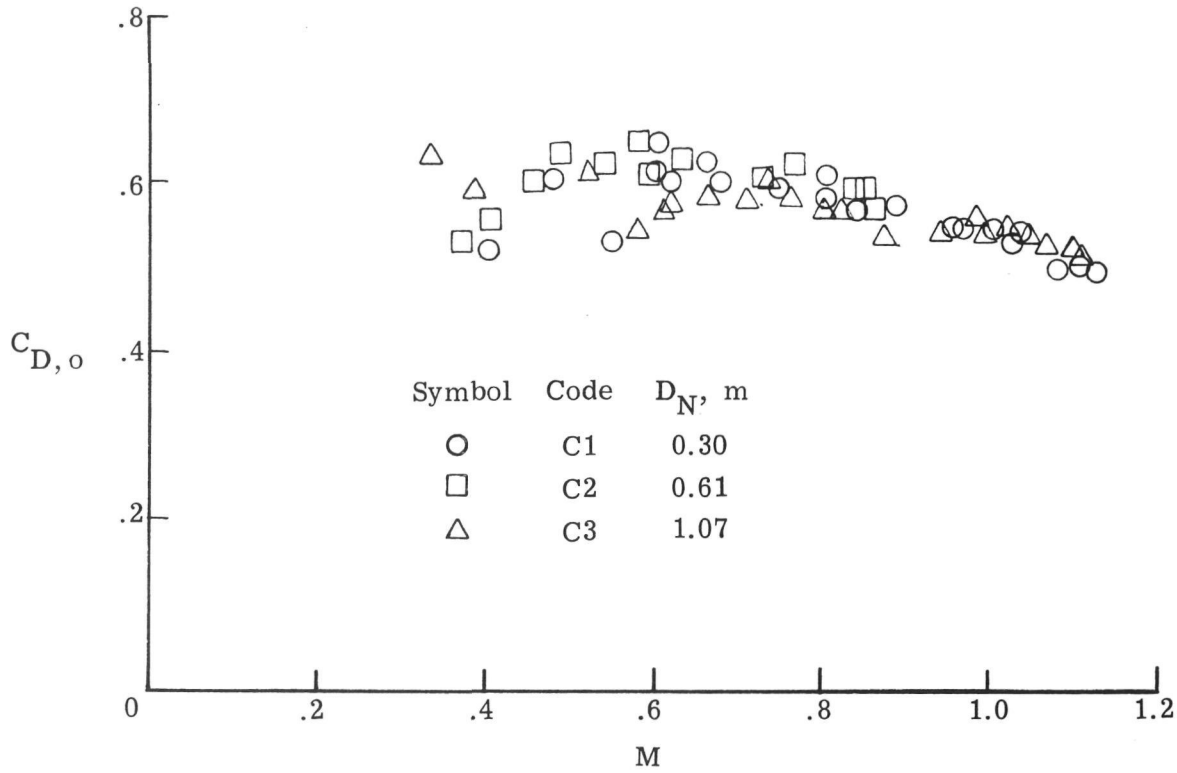

Figure 4.- Variation of drag coefficient with Mach number for modified cross parachute. (Panel length used for reference diameter.)

(a) Test code C1
D_N = 0.30 m
M = 1.11
q = 2250 N/m^2 (47 lbf/ft^2)
$C_{D,o}$ = 0.50

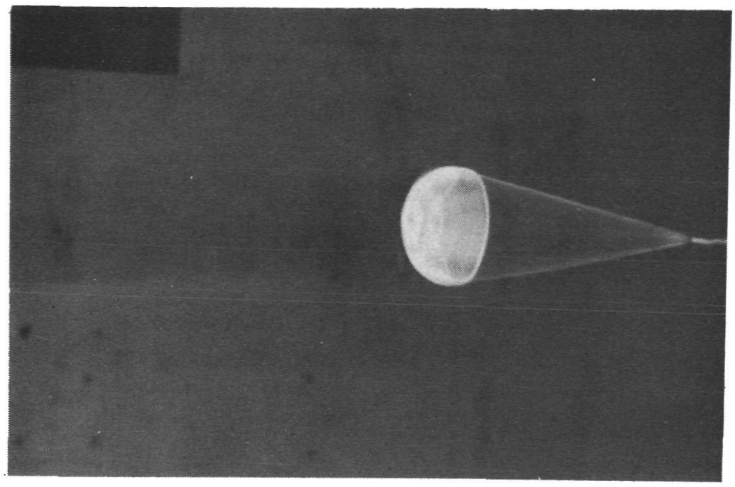

(b) Test code C2
D_N = 0.61 m
M = 0.49
q = 1053 N/m^2 (22 lbf/ft^2)
$C_{D,o}$ = 0.64

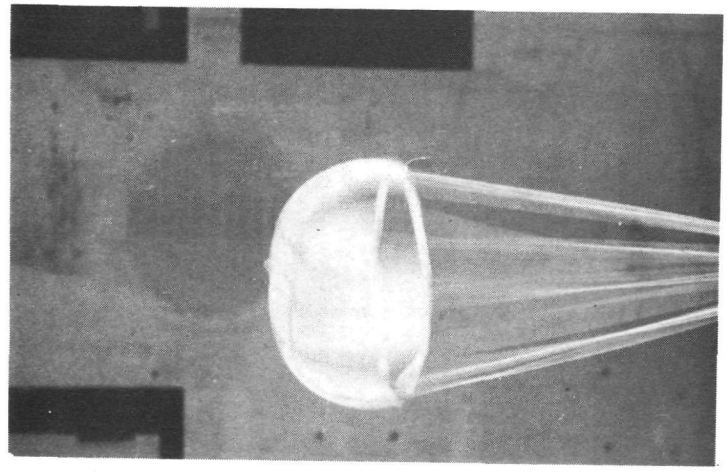

(c) Test code C3
D_N = 1.1 m
M = 0.34
q = 527 N/m^2 (11 lbf/ft^2)
$C_{D,o}$ = 0.63

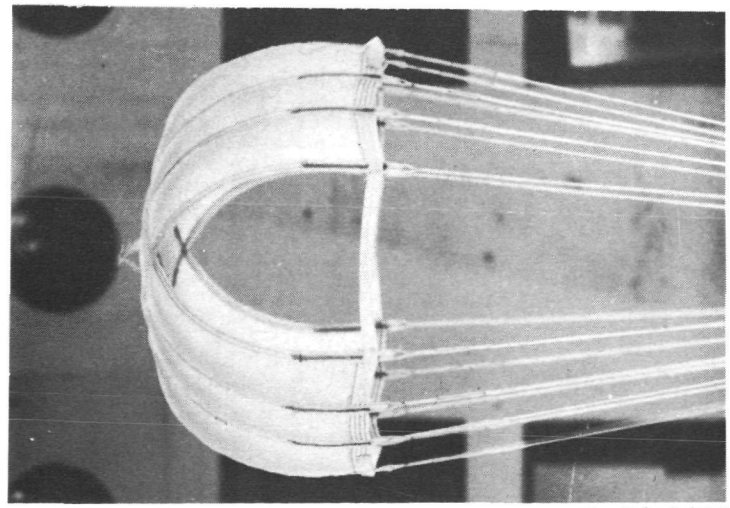

L-74-1155

Figure 5.- Representative modified cross parachute photographs.

(a) Test code C3
M = 0.34
$q = 527\ N/m^2$ (11 lbf/ft^2)
$C_{D,o} = 0.63$

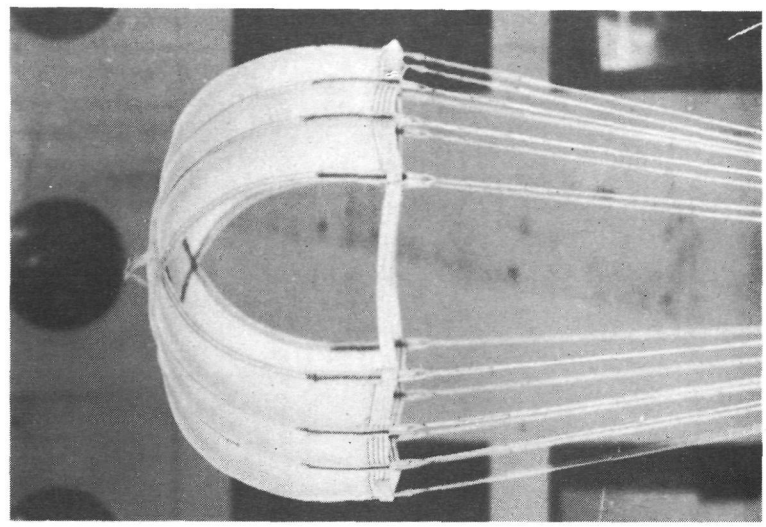

(b) Test code C3
M = 0.77
$q = 2250\ N/m^2$ (47 lbf/ft^2)
$C_{D,o} = 0.58$

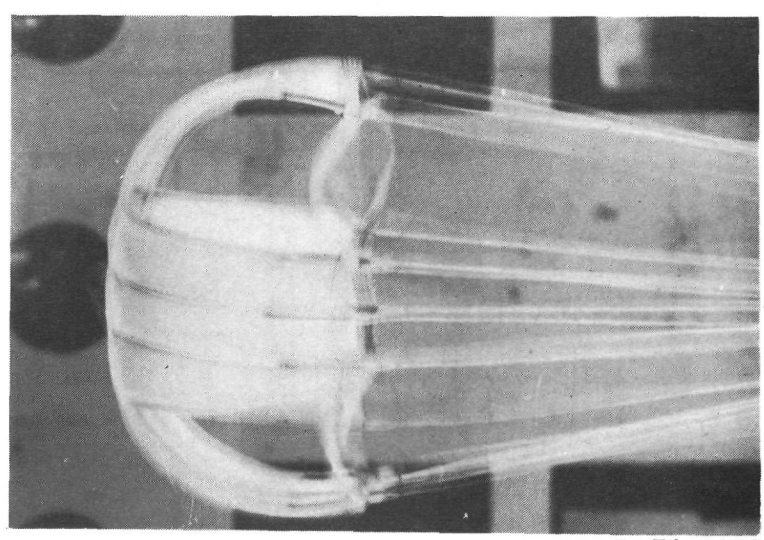

L-74-1156

Figure 6.- Inflated shape and size change for 1.07-meter-diameter model cross parachute.

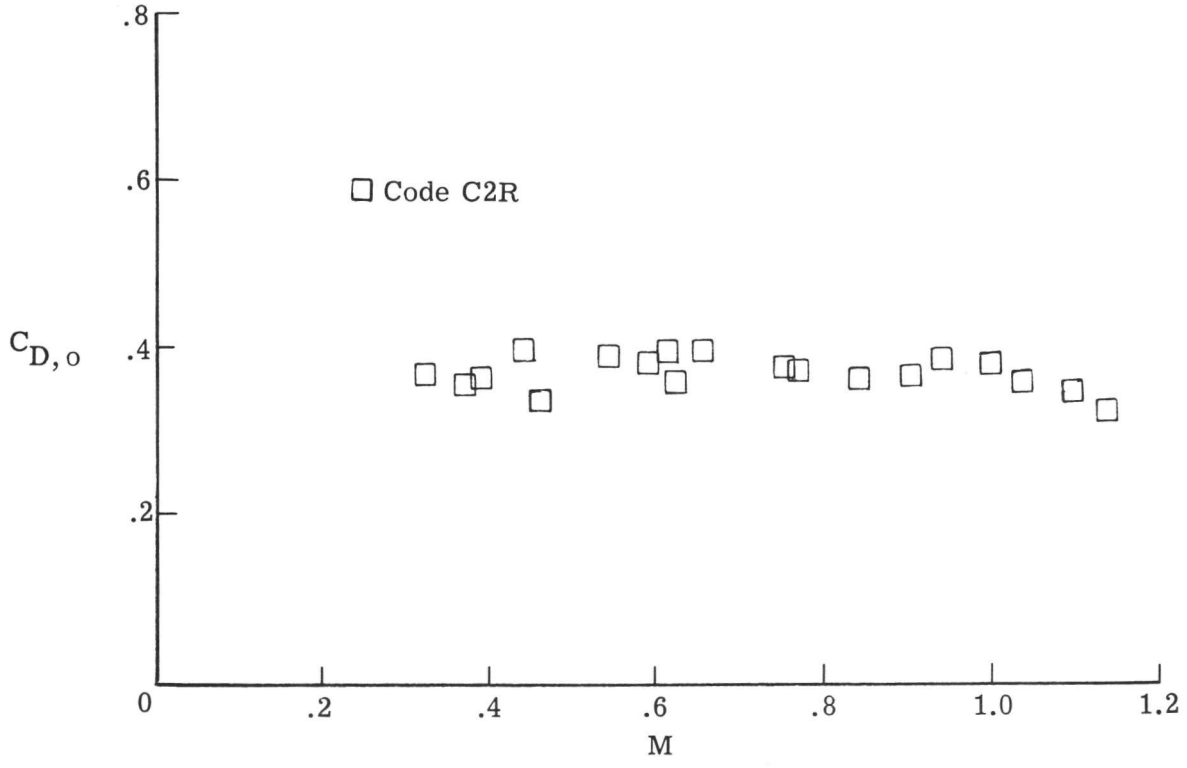

Figure 7.- Variation of drag coefficient with Mach number for reefed cross parachute. (Panel length used for reference diameter.)

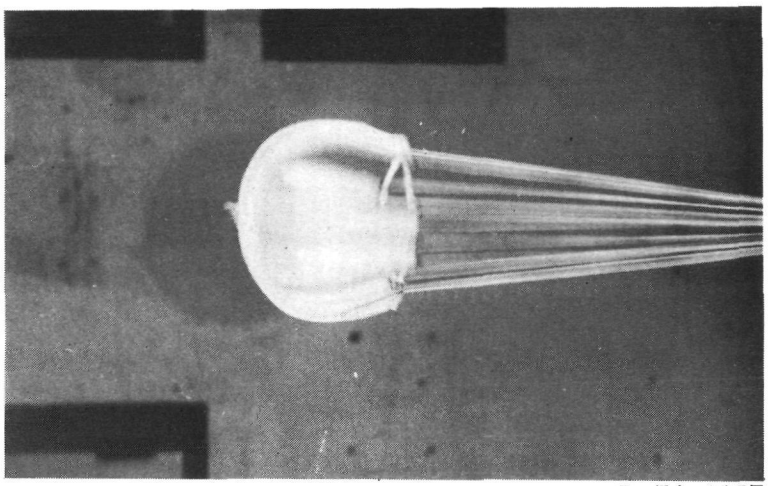

L-74-1157

M = 0.46

q = 2346 N/m^2 (49 lbf/ft^2)

$C_{D,o}$ = 0.33

Figure 8.- Representative photograph of a code C2R reefed cross parachute.

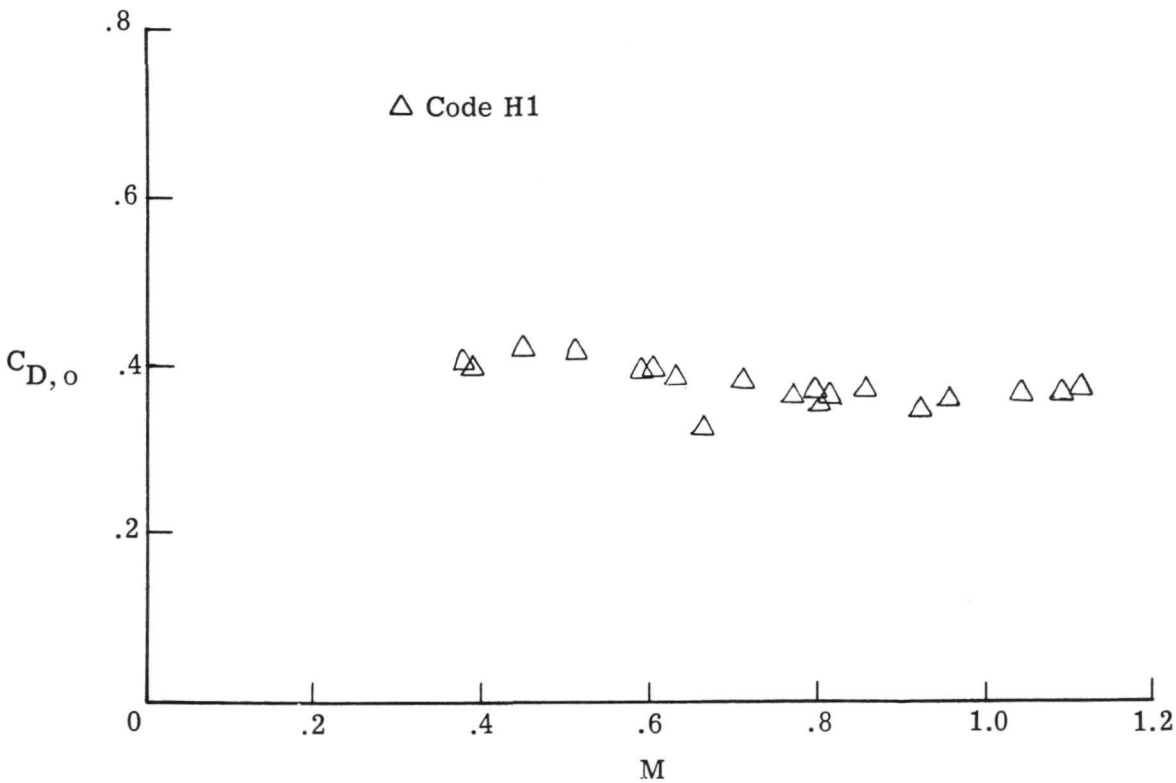

Figure 9.- Variation of drag coefficient with Mach number for hemisflo parachute.

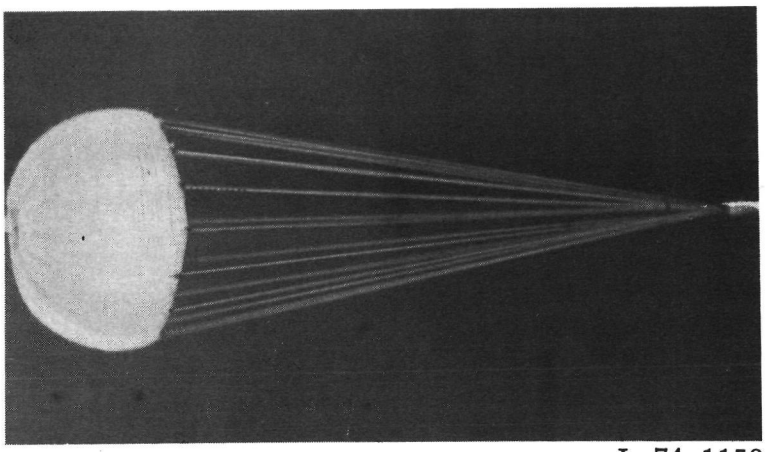

L-74-1158

M = 0.80

q = 3591 N/m^2 (75 lbf/ft^2)

$C_{D,o}$ = 0.35

Figure 10.- Representative photograph of code H1 hemisflo parachute.

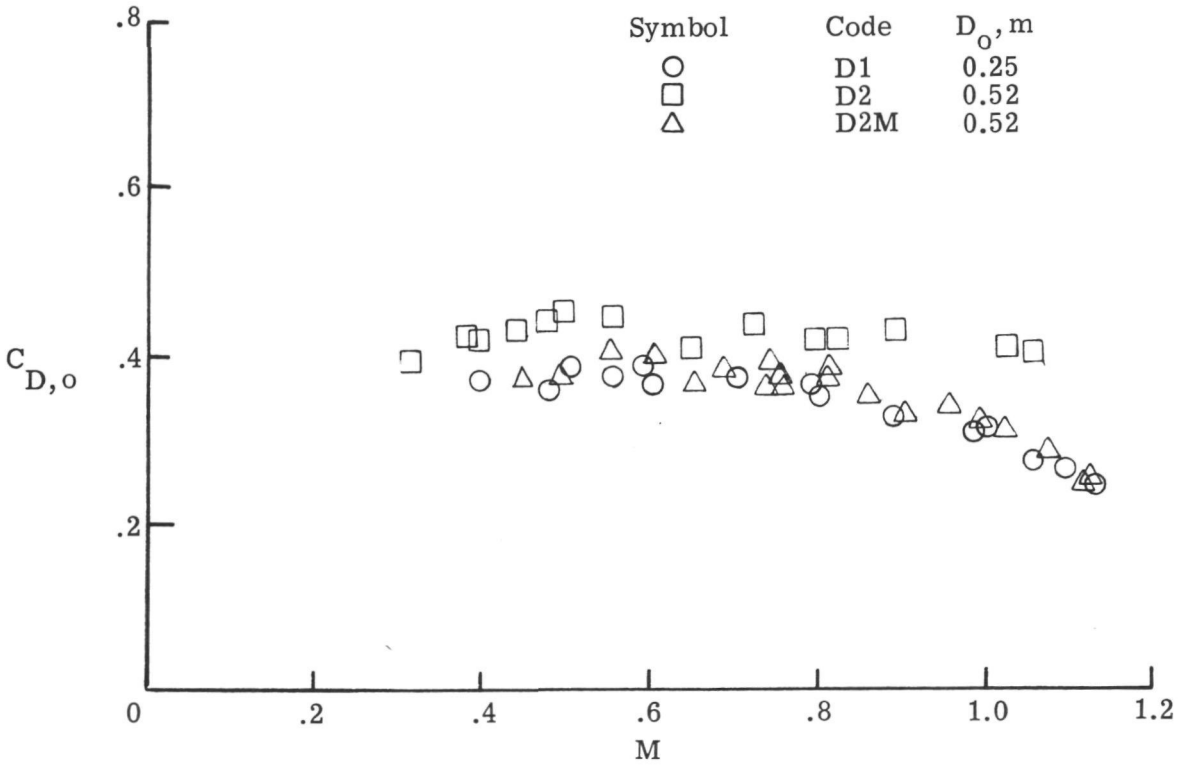

Figure 11.- Variation of drag coefficient with Mach number for disk-gap-band parachute.

(a) Test code D1

D_o = 0.25 m

M = 0.59

q = 2250 N/m^2 (47 lbf/ft^2)

$C_{D,o}$ = 0.39

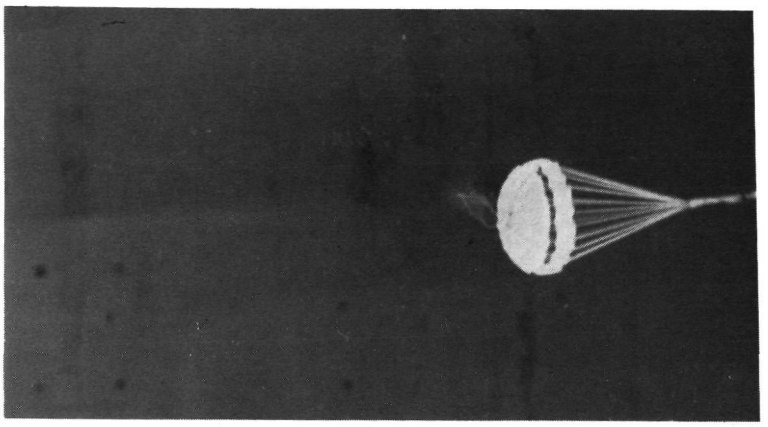

(b) Test code D2

D_o = 0.52 m

M = 1.06

q = 5458 N/m^2 (114 lbf/ft^2)

$C_{D,o}$ = 0.40

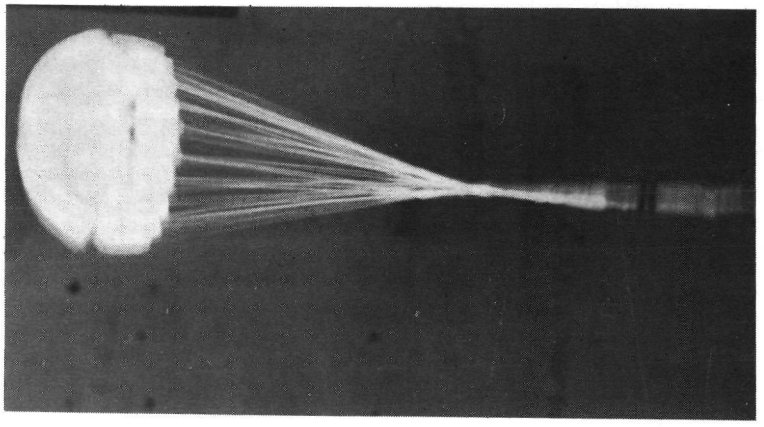

(c) Test code D2M

D_o = 0.52 m

M = 0.60

q = 2442 N/m^2 (51 lbf/ft^2)

$C_{D,o}$ = 0.40

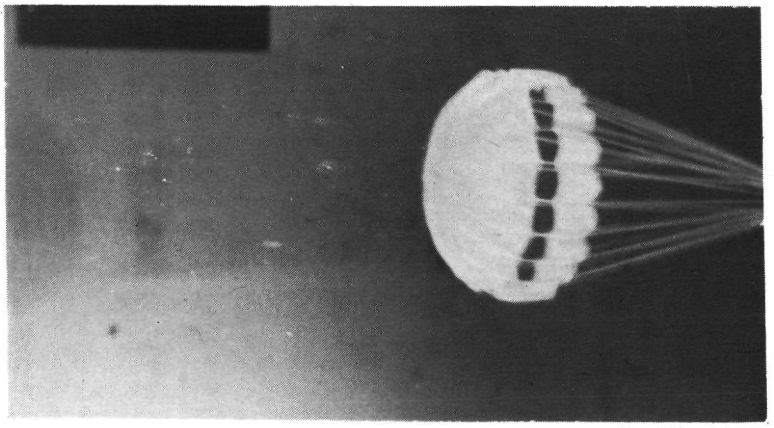

L-74-1159

Figure 12.- Representative photographs of disk-gap-band parachutes.

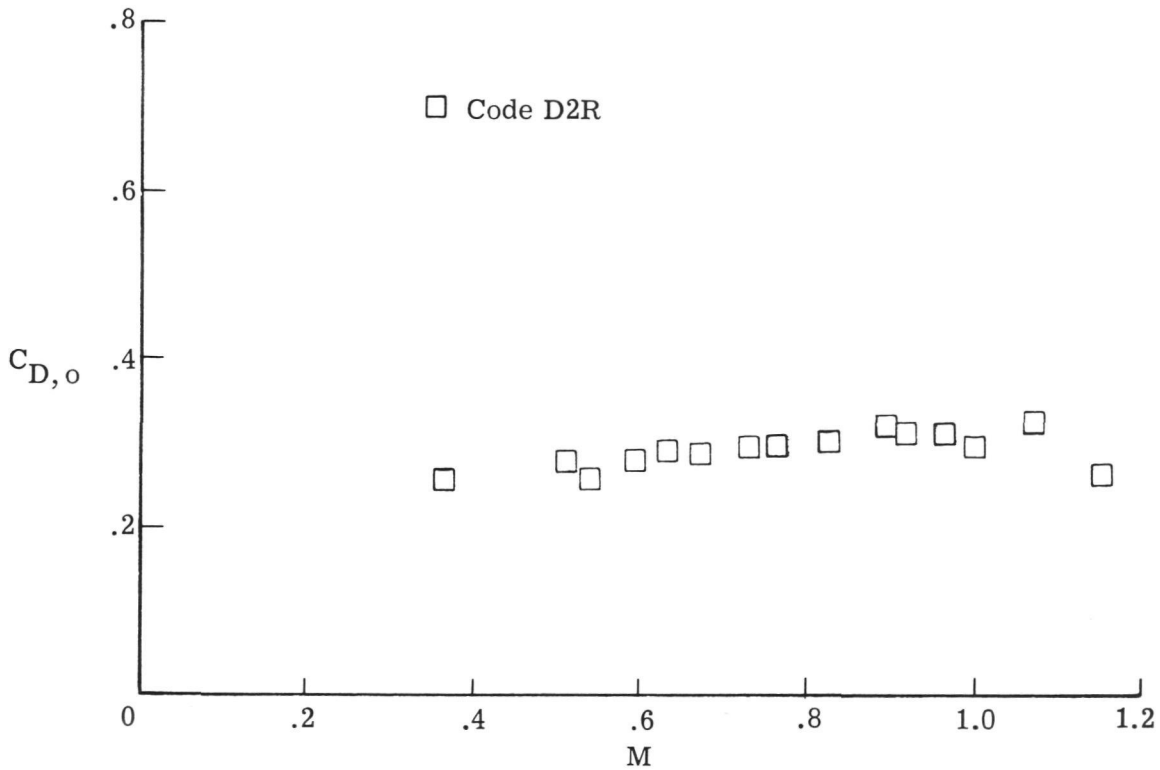

Figure 13.- Variation of drag coefficient with Mach number for reefed disk-gap-band parachute.

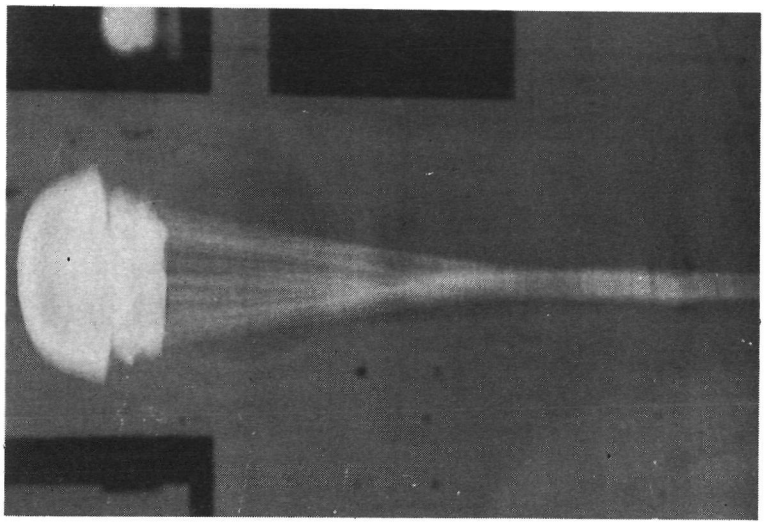

L-74-1160

M = 1.00

$q = 3160\ N/m^2$ (66 lbf/ft^2)

$C_{D,o} = 0.30$

Figure 14.- Representative photograph of a code D2R reefed disk-gap-band parachute.

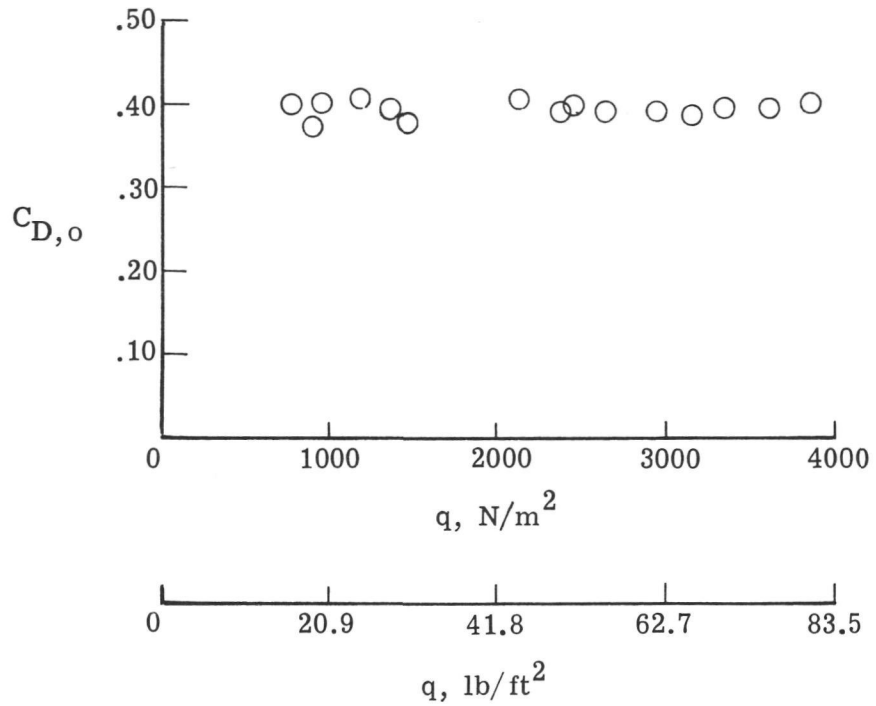

(a) Variation with dynamic pressure.

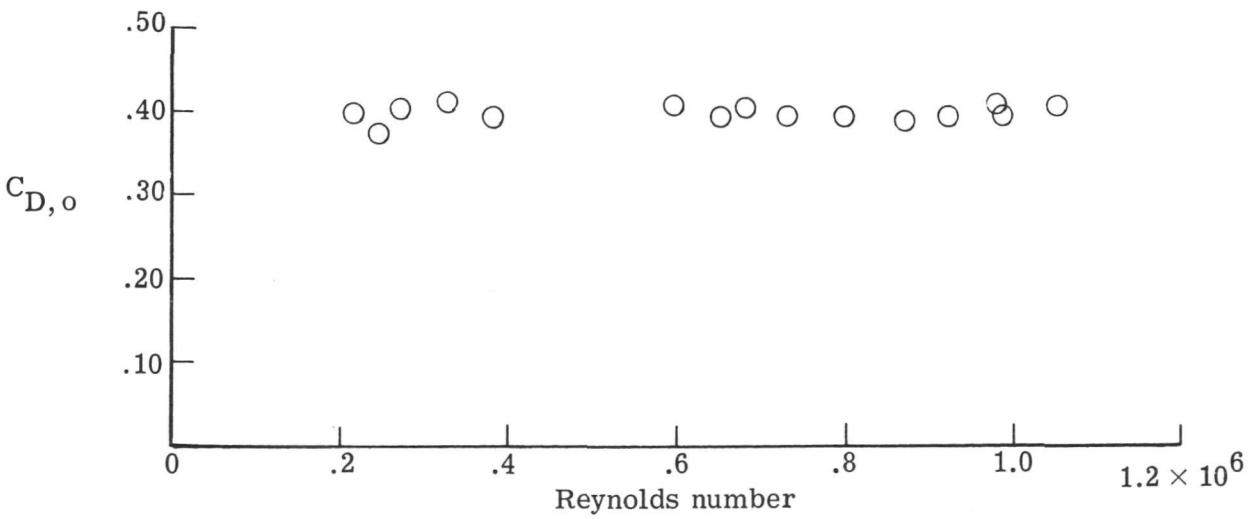

(b) Variation with Reynolds number (length equals 0.52 meter).

Figure 15.- Effect of dynamic pressure and Reynolds number on drag coefficient at Mach 0.6 (disk-gap-band parachute, code D2M).

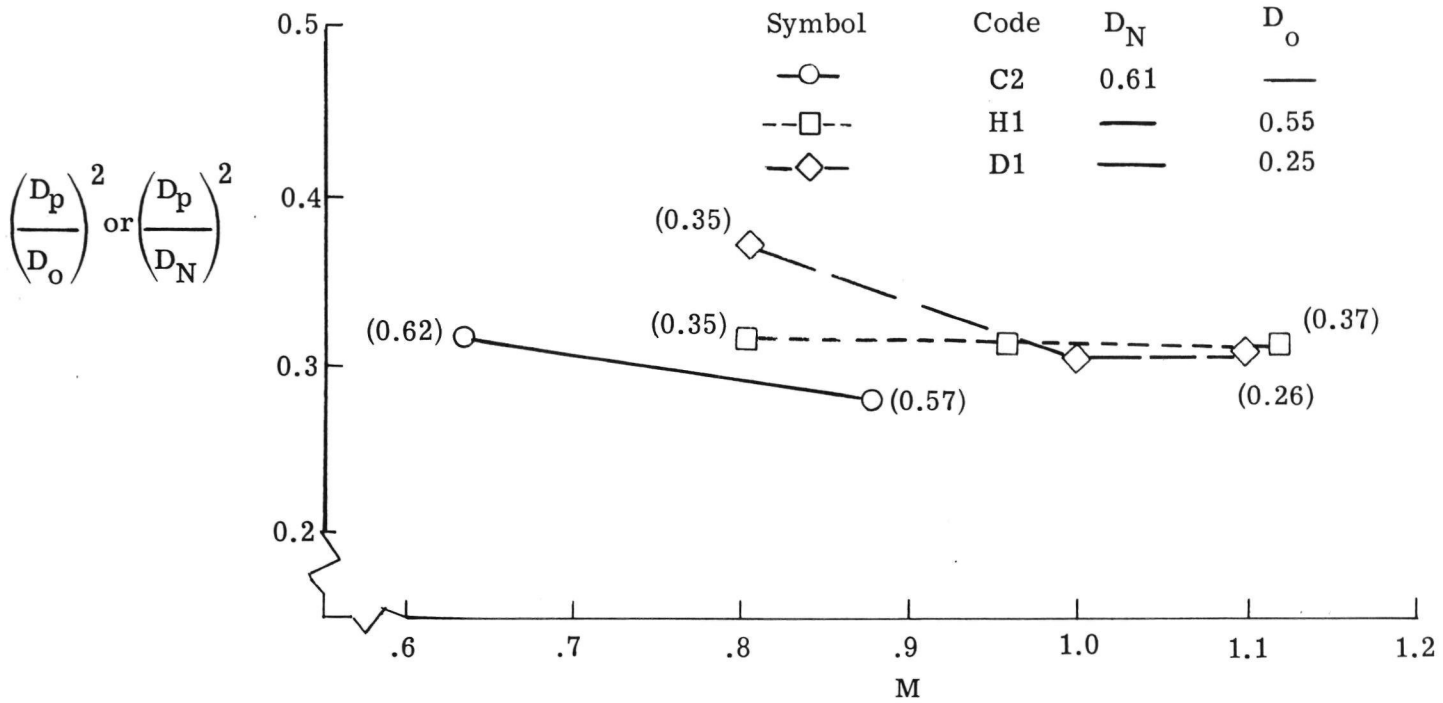

Figure 16.- Variation of projected diameter squared to reference or nominal diameter squared in the transonic range (drag coefficient values shown in parentheses).

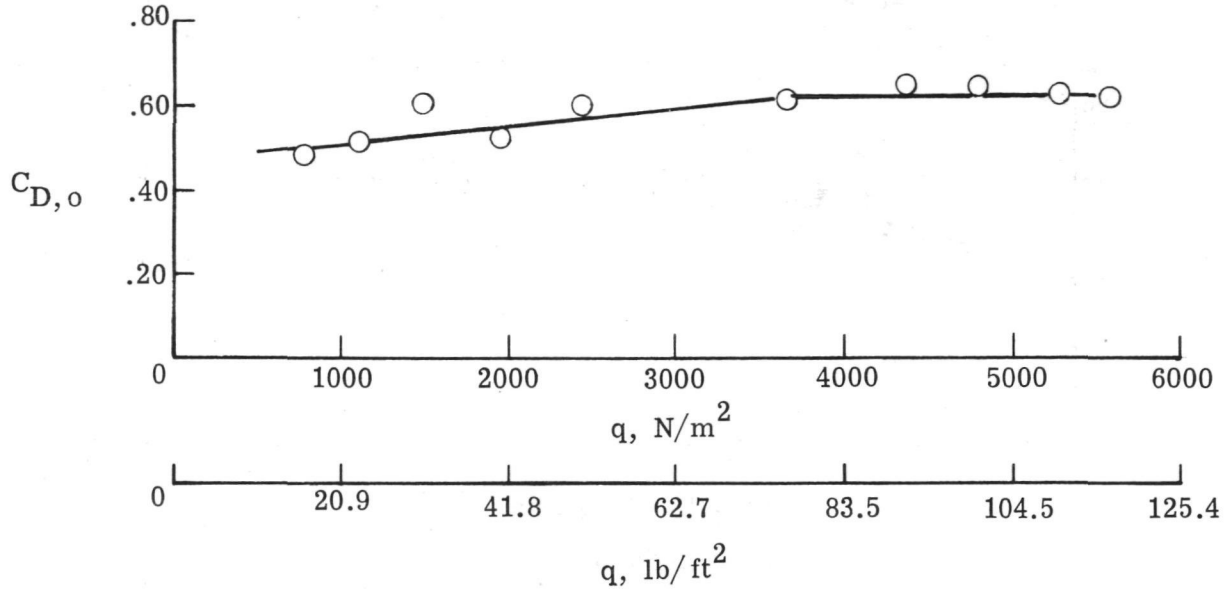

(a) Code C1, 0.30-meter-diameter model.

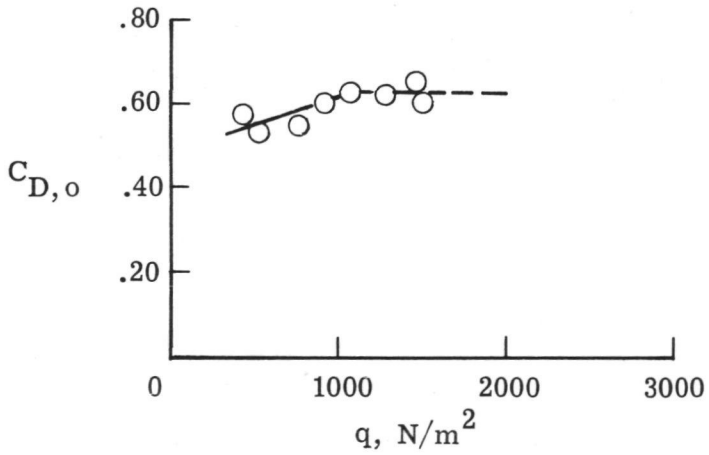

(b) Code C2, 0.61-meter-diameter model.

Figure 17.- Modified cross parachute drag performance as function of dynamic pressure. Mach number, 0.3 to 0.6.

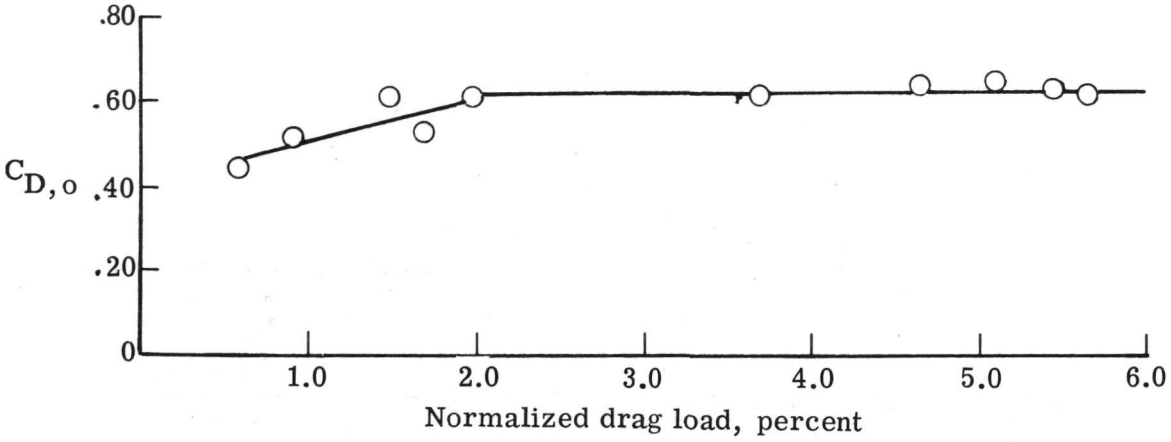

(a) Code C1, 0.30-diameter model.

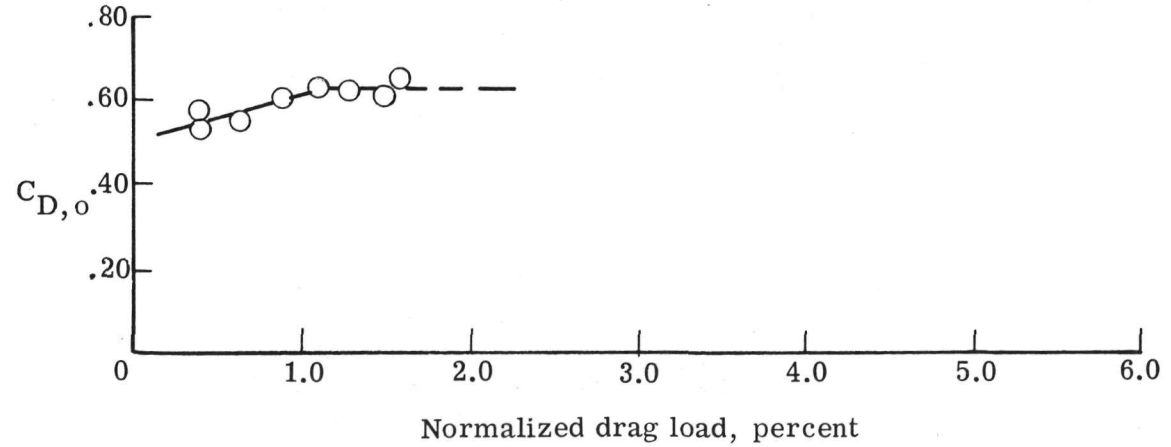

(b) Code C2, 0.61-diameter model.

Figure 18.- Normalized drag load for two modified cross models (normalized drag load equals load divided by rated strength of suspension lines times number of lines).

NASA-Langley, 1974 L-9421

"The aeronautical and space activities of the United States shall be conducted so as to contribute . . . to the expansion of human knowledge of phenomena in the atmosphere and space. The Administration shall provide for the widest practicable and appropriate dissemination of information concerning its activities and the results thereof."

—NATIONAL AERONAUTICS AND SPACE ACT OF 1958

NASA SCIENTIFIC AND TECHNICAL PUBLICATIONS

TECHNICAL REPORTS: Scientific and technical information considered important, complete, and a lasting contribution to existing knowledge.

TECHNICAL NOTES: Information less broad in scope but nevertheless of importance as a contribution to existing knowledge.

TECHNICAL MEMORANDUMS: Information receiving limited distribution because of preliminary data, security classification, or other reasons. Also includes conference proceedings with either limited or unlimited distribution.

CONTRACTOR REPORTS: Scientific and technical information generated under a NASA contract or grant and considered an important contribution to existing knowledge.

TECHNICAL TRANSLATIONS: Information published in a foreign language considered to merit NASA distribution in English.

SPECIAL PUBLICATIONS: Information derived from or of value to NASA activities. Publications include final reports of major projects, monographs, data compilations, handbooks, sourcebooks, and special bibliographies.

TECHNOLOGY UTILIZATION PUBLICATIONS: Information on technology used by NASA that may be of particular interest in commercial and other non-aerospace applications. Publications include Tech Briefs, Technology Utilization Reports and Technology Surveys.

Details on the availability of these publications may be obtained from:

SCIENTIFIC AND TECHNICAL INFORMATION OFFICE

NATIONAL AERONAUTICS AND SPACE ADMINISTRATION

Washington, D.C. 20546